Sustainable proliferation of liposomes compatible with inner RNA replication

Gakushi Tsuji[a], Satoshi Fujii[b,c], Takeshi Sunami[b,d], and Tetsuya Yomo[a,b,c,1]

[a]Graduate School of Frontier Biosciences, Osaka University, 1-3 Yamadaoka, Suita, Osaka, 565-0871, Japan; [b]Dynamical Micro-Scale Reaction Environment Project, Exploratory Research for Advanced Technology, Japan Science and Technology, 1-5 Yamadaoka, Suita, Osaka, 565-0871, Japan; [c]Graduate School of Information Science and Technology, Osaka University, 1-5 Yamadaoka, Suita, Osaka, 565-0871, Japan; and [d]Institute for Academic initiatives, Osaka University, 1-1 Yamadaoka, Suita, Osaka, 565-0871, Japan

Although challenging, the construction of a life-like compartment via a bottom–up approach can increase our understanding of life and protocells. The sustainable replication of genome information and the proliferation of phospholipid vesicles are requisites for reconstituting cell growth. However, although the replication of DNA or RNA has been developed in phospholipid vesicles, the sustainable proliferation of phospholipid vesicles has remained difficult to achieve. Here, we demonstrate the sustainable proliferation of liposomes that replicate RNA within them. Nutrients for RNA replication and membranes for liposome proliferation were combined by using a modified freeze–thaw technique. These liposomes showed fusion and fission compatible with RNA replication and distribution to daughter liposomes. The RNAs in daughter liposomes were repeatedly used as templates in the next RNA replication and were distributed to granddaughter liposomes. Liposome proliferation was achieved by 10 cycles of iterative culture operation. Therefore, we propose the use of culturable liposomes as an advanced protocell model with the implication that the concurrent supplement of both the membrane material and the nutrients of inner reactions might have enabled protocells to grow sustainably.

protocell | freeze–thaw | flow cytometry | liposome fusion

Reconstitution of living cell-like compartments via a bottom–up approach using only well-defined components has remained a challenge in the expansion of our understanding of the possible origin of life, the border between living and nonliving matter, and the use of such compartments in other applications (1–3). Two of the requirements to reconstitute cell growth are the proliferation of compartments (4) and the replication of genetic information (5). These reactions should be sustainable to prevent the extermination of life. Artificial cell models in which phospholipid or fatty acid vesicles encapsulate the replication reactions of genetic information and other biochemical reactions have been proposed (6–10). In addition to replicating RNA/DNA internally, vesicle compartments should grow and divide to proliferate. Fatty acids transform among monomers, small micelles, and enclosed vesicles by changing the pH of the solution (11). The flexibility of fatty acids enables the exchange of fatty acids between vesicles and monomers, reconstituting the model of vesicle "growth" and also "division" into daughter vesicles by shear forces (12, 13). Fatty acid vesicles could continuously grow and divide in a primitive environment, compatible with internal RNA replication (12, 14). However, because phospholipids lack flexible dynamics compared with fatty acids, the coupled growth and division of liposomal artificial cells has been difficult to achieve (15). Because modern cells are composed of phospholipids, which have been proposed to be transited from protocells composed of fatty acids (16), artificial cells composed of phospholipids should be developed to create a valid model. As an attempt to reconstitute liposomal cell growth, phospholipid synthesis (17–20) and liposome division (21) have been reported individually but have not been integrated. Temporal liposome reproduction linked with internal DNA replication has been achieved by supplying membrane precursors and birthing daughter liposomes (22). However, the

daughter liposomes were not continuously birthed due to nutrient depletion and gradual changes in lipid composition.

In this study, we aimed to reconstitute a protocell model that can be continuously "cultured." We fused liposomes containing NTPs and RNA-replicase (nutrient liposomes) with liposomes in which RNA was encapsulated (RNA liposome). We expected that the fusion of the RNA and nutrient liposomes would result in spontaneous fission due to the excess ratio of membrane area to volume (23). Liposome fusion has been achieved using many materials, such as polyethylene glycol (24), amphiphilic molecules (25), cationic ions (26, 27), peptides (28), or lipid-anchored DNA oligonucleotides (29). However, because these systems require the addition of chemical compounds or peptides, the properties of the lipid membranes and/or biochemical reactions will change and may not maintain the same conditions after liposome fusion. To reconstitute sustainable artificial cell growth, lipid composition and inner biochemical reactions should be recursively maintained. Therefore, we developed a method to fuse liposomes without the addition of chemical compounds. The freeze–thaw (F/T) technique has been well-studied as a method to encapsulate drugs into liposomes and to fuse liposomes (30, 31). We modified the F/T method to fuse nutrient liposomes with RNA liposomes.

Using the F/T technique, we observed lipid mixing, followed by the spontaneous fission of liposomes. Simultaneously, we observed the content mixing of liposomes, enabling RNA replication in liposomes. The replicated RNA was distributed to the divided daughter liposomes and used as the template in the next replication reaction. We iteratively repeated this supplementation with nutrient liposomes 10 times and demonstrated the sustainable proliferation of liposomes replicating their RNA. These culturable liposomes suggest

Significance

The reconstitution of liposomal growth and division compatible with replication of genetic information are required for the development of model cell growth. The growth dynamics of liposomes and their internal reactions should be synchronized to maintain the whole system. In this report, we demonstrate the concurrent incorporation of nutrients and membranes into RNA-containing liposomes using a modified freeze–thaw technique. The fusion and fission of liposomes, RNA replication, and distribution to daughter liposomes were observed compatibly. Finally, the sustainable proliferation of RNA-containing liposomes was observed by iteratively supplying nutrients for 10 cycles. We propose the use of this culturable liposome as an advanced recursive model of a liposomal protocell.

that the concurrent supplementation of the membrane material and the nutrients of the inner reactions are a plausible method by which protocells grew on the early earth.

Results

Fusion and Fission of Liposomes. We developed an F/T method to fuse liposomes. We used a water-in-oil (w/o) emulsion transfer method to prepare giant unilamellar vesicles (GUVs) (32) as the model compartments. GUVs resemble living cells in their size and lamellarity and are therefore frequently used as a model of artificial cells (33, 34). Drug delivery research has demonstrated that liposomes can be fused when F/T-ed in liquid nitrogen (30, 31). We confirmed that the liposomes constructed in our experiment could also be fused by F/T (Fig. 1*A*). We prepared two solutions of liposomes using 1-Palmitoyl-2-oleoyl-sn-glycero-3-phosphocholine (POPC) and lipids probed with ATTO 633 (ATTO633; L1) or ATTO 565 (ATTO565; L2). Transferrin protein conjugated with Alexa Fluor 488 (TA488) was encapsulated in both liposomes as a fluorescent content marker. We then mixed those liposome solutions in a concentration ratio of 1:1 and centrifuged the mixture to produce a liposomal pellet to increase the fusion efficiency. Next, we placed the tube into liquid nitrogen without dissolving the pelleted liposomes. We predicted that the inner contents of the liposomes would leak after thawing, and we therefore centrifuged and replaced the supernatant with fresh buffer and measured the liposome fluorescence by flow cytometry (FCM) (Fig. 1*B*). Liposome fusion would result in mixing of the lipid fluorescent markers, which would be detectable by FCM. We did not observe significant lipid mixing before (L1, L2) or after liposomes were mixed (mix) or even after centrifugation (centrifuge). However, after F/T, many liposomes possessed both fluorescent lipid markers, which suggests that lipids were mixed by F/T. Liposomes probed with both fluorescent lipid markers were constructed and measured as the positive control (P.C.). FCM analysis cannot distinguish fused liposomes from aggregated liposomes because they are both detected as particles emitting both ATTO633 and ATTO565 fluorescence. Therefore, we observed F/T liposomes by confocal microscopy and confirmed that lipids were mixed in liposomal membranes (Fig. 1*C*). The mixing of inner contents was also confirmed by another approach, as shown in Fig. S1. Briefly, two liposomes encapsulating different fluorescent content markers were constructed and subjected to F/T. Most of the resulting liposomes contained both fluorescent content markers. These results demonstrate that F/T can be used to fuse liposomes.

Following liposomal fusion, we expected the fission of liposomes, as has been observed for liposomes fused by other methods (23). To confirm liposome fission, we analyzed the size distribution of liposomes. We prepared liposomes labeled with a fluorescent lipid marker (ATTO390) and an encapsulated fluorescent content marker (TA488). We then subjected the liposome solution to F/T without mixing with the other series of liposome solutions and performed FCM analysis (Fig. 2*A*). Histograms of the fluorescent lipid marker ATTO390 representing liposomal sizes were constructed (Fig. 2*B*). The average decreased by 28.4% after F/T, but the peak position did not change. This indicates that fission or rupture frequently occurred in large liposomes. This is consistent with the microscopic images (Fig. 1*C*). As we describe hereafter, the peak position did not change after the second F/T. Because liposome fusion was demonstrated previously (Fig. 1), the stable size distribution of the liposomes after F/T implies the spontaneous fission of liposomes. Next, we analyzed the effect of the fusion–fission of liposomes by F/T on other parameters. The height of the histograms, which represented liposome concentration (liposomes detected in 1 μL of solution by FCM), decreased 48% after F/T, which indicated that approximately half of the liposomes were ruptured. We then analyzed content leakage by constructing the histograms of the fluorescent content marker TA488 (Fig. 2*C*). The fluorescence intensity of the main peak decreased by 50%, indicating that F/T resulted in the leakage of half of the inner content. In this analysis, we observed an increase in the minor population (arrow in Fig. 2*C*) that did not emit significant TA488 fluorescence. This population may not encapsulate sufficient aqueous solution for use as a cell model compartment. We refer to this population as "inactive liposomes" hereafter; this population was considered to have no influence on the conclusion in this study. These results confirmed the successful reconstitution of the growth and fission of liposomes.
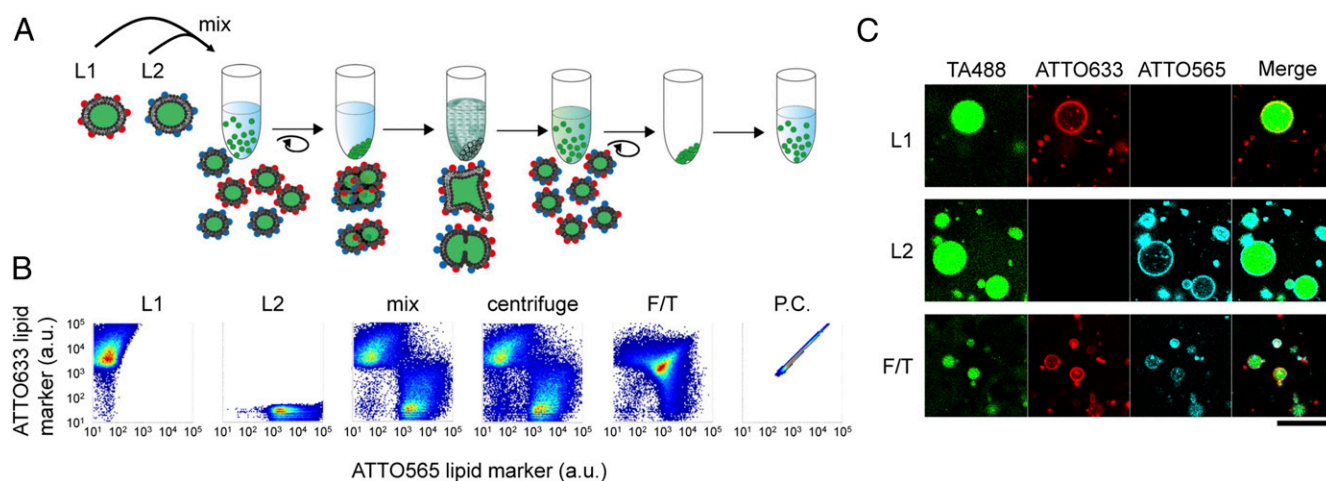
Fig. 1. Lipid mixing of liposomes by the F/T method. (*A*) Experimental procedure for liposome fusion by F/T. Two liposome solutions were mixed (L1 and L2), centrifuged, and subjected to F/T using liquid nitrogen. The liposomes were centrifuged again, and the supernatant was replaced with fresh buffer. Fused liposomes possessed both the fluorescent lipid markers ATTO565 and ATTO633. (*B*) 2D plots of fluorescent lipid markers measured by FCM. Two liposome solutions (L1 and L2) were analyzed before mixing, after mixing (mix), after centrifugation (centrifuge), and after F/T. Liposomes including both fluorescent lipid markers were constructed as a P.C. The horizontal axis shows the fluorescence of ATTO565, and the vertical axis shows the fluorescence of ATTO633. (*C*) Confocal microscopic images of liposomes before mixing (*Upper*, L1; *Middle*, L2) and after F/T (*Lower*, F/T). Fluorescence of TA488, ATTO633, and ATTO565 and the merged images are shown. (Scale bar, 25 μm.)
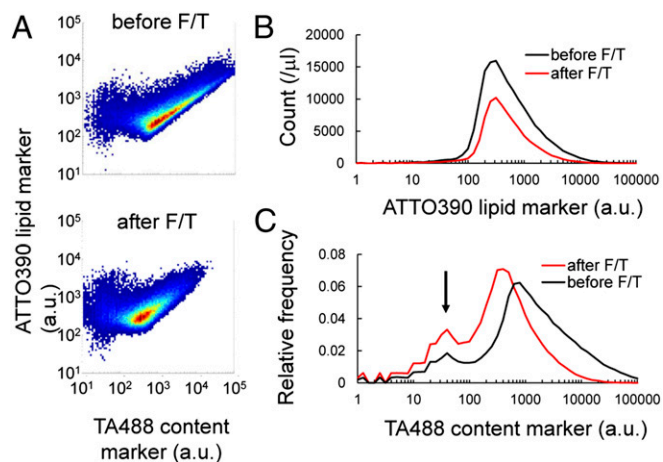
Fig. 2. Size distribution and content leakage of liposomes before (before F/T) and after freeze-thaw (after F/T). (A) 2D plots of liposome fluorescence before and after F/T. The horizontal axis shows TA488 content marker fluorescence, and the vertical axis shows ATTO390 lipid marker fluorescence. (B) Histogram of ATTO390 lipid marker fluorescence. The vertical axis shows the liposome number measured by FCM in 1 μL of liposome solution. (C) Histogram of TA488 content marker fluorescence. The arrow indicates the particles without significant aqueous content. The vertical axis shows the relative frequency.

RNA Replication in Liposomes. RNA was replicated in liposomes by supplying nutrients and using the F/T method. The reconstitution of the fusion and fission of liposomes must be compatible with the replication of genetic information in liposomes. As a model for an RNA replication system, we used a modified midivariant RNA encoding a modified Qβ-replicase (Rep-RNA) in the replication reaction (35) and supplied NTPs and Qβ-replicase for nutrients. We subjected liposomes encapsulating Rep-RNA (RNA liposome) and liposomes encapsulating the NTPs and Qβ-replicase (nutrient liposome) to F/T at a concentration of 1:1 (Fig. 3A). To remove the leaked Rep-RNA, NTPs, and Qβ-replicase, we centrifuged the liposomes, replaced the outer solution with fresh buffer, and incubated the solution at 37 °C for 1 h to replicate Rep-RNA in liposomes. These steps ensured that Rep-RNA replication proceeded only inside the liposomes. Then, we added SYBR Green II, which permeates the lipid membrane and emits fluorescence when RNA molecules are present in liposomes. We preliminarily confirmed the linear relationship between the Rep-RNA concentration

in liposomes and SYBR fluorescence measured by FCM (Fig. S2). We analyzed RNA replication by measuring SYBR fluorescence using FCM (Fig. 3). In this study, we defined liposomes emitting SYBR fluorescence >200 fluorescence intensity (F.I.) as "active liposomes" (green dots in Fig. 3A) in which RNA replicated significantly. Note that liposomes before RNA replication did not emit green fluorescence due to their low initial RNA concentration. After the 1-h RNA replication reaction, 30% of the liposomes were active when mixed with nutrient liposomes (+nutrient), but only 1% were active when nutrient liposomes did not contain NTPs and Qβ-replicase (−nutrient). Nutrient liposomes that lack NTPs or Qβ-replicase also did not generate active liposomes (Fig. S3). We also quantified the RNA in liposomes by sorting the liposomes followed by quantitative reverse transcription PCR (qRT-PCR) and confirmed that RNA was replicated in liposomes (Fig. S2C). Some liposomes, indicated by white arrows in Fig. 3B, did not exhibit SYBR fluorescence and corresponded to liposomes less than 200 F.I. in the FCM analysis (black dots in Fig. 3A). These liposomes were considered to be inactive liposomes that do not replicate RNA internally. These liposomes could have originated from liposomes that lost aqueous solution, as shown before (black arrow in Fig. 2C). These results demonstrate that sufficient nutrients for RNA replication can be supplied from nutrient liposomes to RNA liposomes by F/T.

Distribution of RNA to Daughter Liposomes. Next, we tested whether the replicated RNA could be distributed to the daughter liposomes. We mixed a constant volume of RNA liposome solutions with nutrient liposomes at ratios of 1:1 and 1:99 (Fig. 4). After the first F/T and RNA replication, the distribution of the RNA molecules to more than two daughter liposomes by the second F/T and RNA replication reaction would result in an increase in the number of liposomes with significant SYBR fluorescence (active liposomes). After the first F/T and RNA replication for 2 h, the proportions of active, RNA-replicating liposomes (green dots in Fig. 4B) were 43% and 12% at mixing conditions of 1:1 and 1:99, respectively. These liposome solutions were again diluted with each mixing ratio and subjected to the second F/T. Thus, 21.5% and 0.12% of the liposomes could have amplified the RNA molecules in the second replication reaction if the RNA was not distributed. However, RNA-replicating liposome populations increased from 21.5% to 47% and 0.12% to 8.3% at mixing conditions of 1:1 and 1:99, respectively. These fold increases imply that single mother liposomes distributed RNA to 2.2 and 69 daughter liposomes at mixing ratios of 1:1 and 1:99, respectively. Excess nutrient liposomes compared with RNA liposomes may have caused the RNA molecules to distribute by
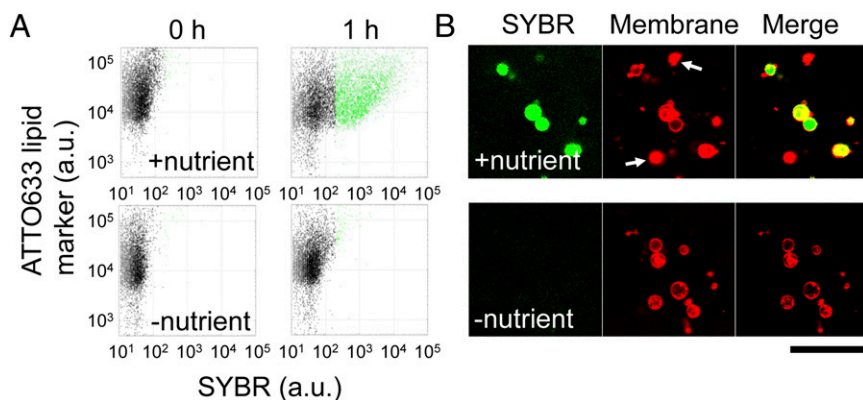
Fig. 3. Induction of RNA replication by F/T. Liposomes encapsulating Rep-RNA were mixed with nutrient liposomes, subjected to F/T, and incubated for 1 h at 37 °C. (A) 2D plots of liposome fluorescence before and after RNA replication. Nutrient liposomes that did not contain NTPs and Qβ-replicase were introduced as a negative control (−nutrient). The horizontal axis shows SYBR fluorescence (RNA content), and the vertical axis shows ATTO633 lipid marker fluorescence. (B) Confocal microscopic images of liposomes after a 1-h incubation. The fluorescence of SYBR, the ATTO633 lipid marker (Membrane), and the merged images are shown. (Scale bar, 25 μm.)
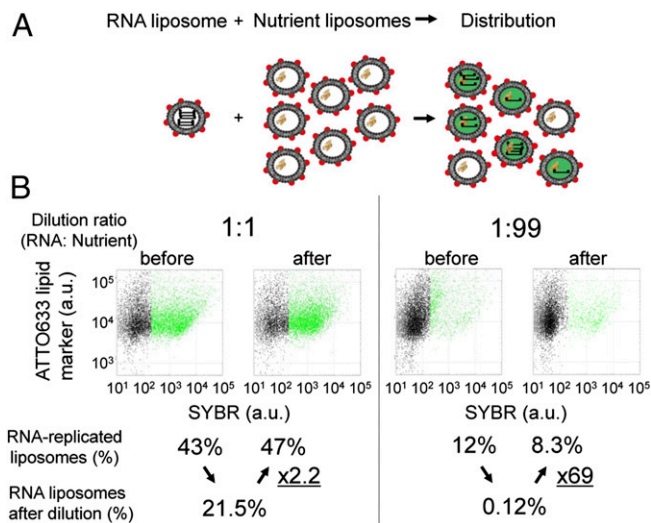
Fig. 4. Distribution of RNA to other liposomes by F/T. (*A*) Schematic of the RNA distribution experiment. RNA liposomes were mixed with an excess ratio of nutrient liposomes, subjected to F/T, and incubated for 2 h at 37 °C. The fold increase in the population ratio of RNA-replicating liposomes represents the distribution rate. (*B*) 2D plots of liposome fluorescence before and after RNA replication following F/T with mixing ratios of RNA:nutrient of 1:1 and 1:99. The horizontal axis shows the fluorescence of SYBR (RNA content), and the vertical axis shows the fluorescence of the ATTO633 lipid marker. Green dots represent the liposomes actively replicating RNA, which exhibit SYBR fluorescence >200 F.I. The population ratios of green dots among all dots in each plot are shown below the plots. Estimated ratios after F/T and RNA replication, assuming no distribution of RNA, are also shown.

single molecules (Fig. 4*A*), therefore resulting in the higher fold increase at the 1:99 mixing ratio. This indicates that at least 69 daughter liposomes can be birthed from a single mother liposome. This may be caused not only by fusion–fission but together with spreading the inner contents via a transient pore, therefore exchanging the nutrients and RNAs among liposomes nearby.

Continuous Cultivation of Active Liposomes. Thus far, we have demonstrated liposome fusion and fission, RNA replication, and

the distribution of RNA to daughter liposomes. Next, we tested whether this system was "sustainable" by repeating the F/T (Fig. 5). We constructed RNA liposomes encapsulating Rep-RNA as the original protocells and nutrient liposomes encapsulating NTPs and Qβ-replicase. Both liposomes were probed with the fluorescent lipid marker ATTO633. We mixed the two liposome solutions at a 1:1 volume ratio, performed F/T, and incubated the liposomes to permit RNA replication. We then repeated the cycle of dilution of the resulting liposome solution with fresh nutrient liposome solution at a 1:1 ratio, F/T, and incubation for 1 h of RNA replication 10 times iteratively (Fig. 5). When we analyzed the liposomes by FCM, SYBR fluorescence was consistently observed until the 10th F/T operation (the horizontal axis in Fig. 5*A*). Thus, RNA replication was not terminated and was sustained by supplying nutrients. This result also indicates that the proliferation of liposomes and the replication of RNA are sustainable for 10 cycles despite the dilution with nutrient liposomes and rupture and leakage by F/T. We performed the first to fourth F/T cycles and the fifth freezing on the first day and then stored the liposome solution at –80 °C for 10 d. We began again from the fifth thawing, fifth RNA replication, and the 6th to 10th F/T cycles. These results demonstrate that active liposomes can be stored with standard laboratory equipment.

We first analyzed the sustainability of liposome size (Fig. 5*B*). The histograms of fluorescent lipid markers did not change significantly during the experiment, which indicates that a stable liposome size was maintained despite repetitive fusion, fission, and rupture by 10 F/T cycles. The majority of the liposomes are expected to contain aqueous volumes of ~10 fL based on our previous reports (36, 37). The lamellarity of the liposomes was not significantly changed by the repetition of F/T (Fig. S4).

We then analyzed the sustainability of active liposome proliferation (Fig. 5*C*). Active liposomes representing liposomes encapsulating significant amounts of RNA increased after 1 h of replication. Dilution with nutrient liposomes and subsequent F/T generated the zigzag plot in Fig. 5*C*. The active ratio after the fifth F/T (left end of red line) did not decrease from the previous data point before the F/T cycle (right end of black line). Thus, the RNA was less diluted by leakage and/or more daughter liposomes were born than in other cycles after the liposomes were frozen for 10 d. The reasons for this effect are unclear. When
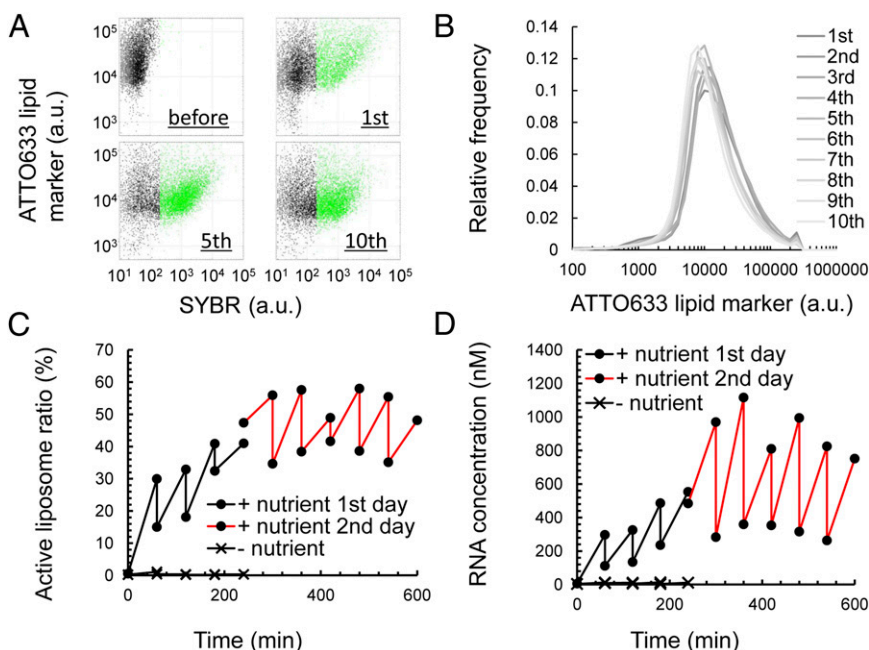
Fig. 5. Repetitive culturing of RNA-replicating liposomes. (*A*) 2D plots of fluorescence measured by FCM. Liposomes (before) were F/T-ed with nutrient liposomes and incubated for 1 h (first). F/T with nutrient liposomes was repeated for 10 cycles. The plots of liposomes incubated after the 5th and 10th F/T are also shown. The horizontal axis shows SYBR fluorescence (RNA content), and the vertical axis shows ATTO633 lipid marker fluorescence. (*B*) Histogram of ATTO633 lipid marker fluorescence after each 1-h incubation period following F/T. (*C*) The population ratios of active liposomes (green dots in *A*) were plotted against the total incubation time. The black and red lines represent data from the first- or second-day experiments, respectively. RNA liposomes were subjected to F/T with liposomes that do not contain NTPs and Qβ-replicase (–nutrient) for five cycles as a negative control. (*D*) RNA concentrations in liposomes were plotted against the total incubation time. Note that the analysis was limited to liposomes with a lipid content of ATTO633 = 8,000–12,000 F.I.

nutrient liposomes did not contain NTPs and Qβ-replicase, the active liposomes were exterminated (–nutrient). Therefore, we observed the sustainable proliferation of RNA-encapsulating liposomes.

We then analyzed the sustainability of RNA replication (Fig. 5D). The average SYBR fluorescence of all liposomes of significant size was converted to the actual Rep-RNA concentration using the equation obtained from the standard curve in Fig. S2. RNA was repeatedly replicated except when nutrient liposomes did not encapsulate NTPs and Qβ-replicase (–nutrient). Therefore, we observed sustainable RNA replication in this system.

Here, we analyzed these data at the molecular and population levels by taking into account the leakage, distribution, and fold replication of RNA. The RNA liposomes initially encapsulated 30 Rep-RNA molecules at a size of 10 fL, following a Poisson distribution. When the first F/T was performed, 50% of the RNA leaked (Fig. 2C), distributed (Fig. S1), and gave birth to 2.2-fold daughter liposomes (Fig. 4). Taking this leakage and the distribution to nutrient liposomes together, the initial RNA concentration before the first replication was expected to decrease fourfold from 5 nM to 1.25 nM. When these liposomes were incubated for 1 h, 297 nM RNA was synthesized (Fig. 5D), suggesting that more than 200-fold RNA was replicated. Next, we analyzed the population of liposomes replicating RNA internally (Fig. 5C). If all liposomes were filled with RNA, all liposomes should replicate RNA. However, because 1.25 nM RNA is below the detection threshold of FCM, the ratio of liposomes with significant SYBR fluorescence was 0.2% at time 0. After replication for 1 h, RNA replication was measured by FCM over the threshold, and the active liposome ratio thus increased to 30% (Fig. 5C). However, even though all liposomes were expected to encapsulate RNA, the active liposome ratio did not reach 100%, possibly because of the presence of inactive liposomes that lacked a significant volume of aqueous solution for the replication reaction to occur (Fig. 2C, black arrow) or liposomes that did not receive the RNAs/nutrients for sufficient RNA replication. Indeed, there were two distinct populations, one that emitted SYBR fluorescence and one that did not, in the FCM analysis (Fig. 5A).

Following the second F/T, RNA was again leaked and distributed, and thus a fourfold dilution of RNA was expected for the next initial RNA concentration. As a result, 112 nM, roughly a threefold dilution of the RNA concentration before F/T (297 nM), was measured as the next initial RNA concentration (Fig. 5D). After 1 h of replication, a threefold increase in RNA (326 nM) was measured. From the second F/T, an approximately threefold dilution and threefold replication were consistently observed until the 10th cycle (Fig. 5D). We then considered why the replication was lower than the first incubation (which was >200-fold). In nutrient liposomes, 6.25 mM NTPs each were encapsulated. These NTPs were also expected to be distributed following the fourfold dilution, as mentioned above. Thus, when we assume 1.56 mM NTPs each were used, the replication of 2,041 bp RNA would terminate at 3,060 nM due to NTP depletion. Because the RNA concentration was on the same order as this upper limitation (the latter half of Fig. 5D), we believe the replication was suppressed by the depletion of NTPs in our experiment. Whereas a fourfold dilution was expected from 50% leakage and 1:1 dilution with nutrient liposomes, a slightly lower threefold dilution was consistently observed. One possible explanation for this discrepancy was that the degree of content leakage decreased after the second F/T due to the loss of large liposomes (Fig. 2B). Next, we analyzed the population of liposomes replicating RNA internally (Fig. 5C). From the second F/T cycle, the ratio gradually increased to 50% and maintained the 50% maximum during the latter half of the cycle experiments (Fig. 5C). This result indicates that inactive liposomes possibly lacking aqueous solution did not exceed 50% and did not dominate the active liposomes.

Together, these data confirm the sustainability of the liposome compartment, RNA replication, RNA distribution, and active liposome proliferation.

Discussion

We reconstituted culturable liposomes that follow fusion–fission and are compatible with a model of RNA replication and RNA diffusion to daughter liposomes. This system requires the supply of nutrient liposomes by the F/T method and thus does not self-grow or self-replicate via the expression of genome information. However, we demonstrated the sustainable proliferation of liposomes with 10 instances of iterative culturing. Although phospholipid membranes are thought to lack the flexible dynamics to grow and divide compared with fatty acids, we demonstrated that concentration and freezing with the supply of nutrient liposomes allowed the RNA liposomes to undergo sustainable proliferation. In addition, we showed that freezing at –80 °C or –20 °C could also cause content mixing, lipid mixing, and RNA replication by supplying nutrients (Fig. S5). All three temperatures showed similar levels of content mixing. However, lipid mixing and RNA replication were highest in liquid nitrogen and lowest at –20 °C. We clarified that the fusion–fission of liposomes compatible with RNA replication was robust at a wide range of freezing temperatures, including the plausible temperature on primitive earth (38). Therefore, with the sustainable proliferation of liposomes compatible with RNA replication, we propose that the concurrent supplementation of the membrane material and the nutrients of the inner reactions are a plausible method by which protocells were able to grow on the early earth (39, 40).

The fusion of liposomes by F/T is thought to be driven by dehydration and ice growth, leading to the disruption of the lipid bilayer (30). Therefore, half of the liposomes were ruptured, and the residual liposomes were used for fusion–fission and RNA replications. Although the details of the volume dependency of fusion, fission, and rupture of liposomes are not clearly understood, a stable size distribution of liposomes during the repetition of F/T was observed. Centrifugation before F/T concentrated the liposomes, which may have enhanced the fusion and exchange rate of inner content. The centrifuged liposomes were able to exchange those inner contents by fusion–fission as shown with lipid mixing (Fig. 1) and possibly by spreading through the transient pore to give birth to more than 69 daughter liposomes (Fig. 4). Observations of the frozen sample before thawing are needed to understand these fusion–fission events in greater detail (30). The majority of the liposomes were expected to contain an aqueous volume of ~10 fL and have a diameter of 2.6 μm, which is similar to the size of living cells and suggests their potential as a good cell model. The volume and diameter will change slightly if we take into account that approximately half of the liposome population is unilamellar (Fig. S4).

Using this system, if we prepare multiple series of nutrient liposomes and fuse these liposomes step by step, multistep reactions in liposomes could be easily reconstituted. Because we can supply lipid membranes, small chemical compounds, and macromolecules (Qβ-replicase), this system would enable the supply of ribosomes or cell-free translation systems (41). As a next step, the encapsulation of cell-free translation systems in liposomes will enable the reconstitution of functionally active liposomes (34, 42) possessing replication activity driven by their own genome products (9). Then, we can introduce additional beneficial functions one by one and culture the artificial cells by iterative F/T steps. To increase the complexity of genomic information, genotype–phenotype linkages should be maintained. In our experiment, if RNA liposomes and nutrient liposomes were mixed at the ratio of 1:1, multiple copies of genomes were encapsulated in single liposomes, giving rise to a weakened genotype–phenotype linkage. To maintain a high selection pressure for individual genomes, we could avoid RNA mixing when excess ratios of nutrient liposomes were supplied (e.g., 1:99). On the other hand, genome mixing could increase the chance for recombination among mutated genes to increase the genetic diversity because the Qβ-replicase has high recombination activity

(43). Future experiments should find the appropriate number of genomes per liposome in the balance of selection pressure and genetic diversity. Thus, these culturable artificial cells would enrich the fittest genotypes among variants, which is the essence of "natural selection" and would enable Darwinian evolution of the liposomal artificial cells.

Materials and Methods

Details of the materials, liposome preparation, FCM analysis, confocal microscopy, and qRT-PCR are provided in *SI Materials and Methods*.

F/T Method for Liposome Fusion–Fission. The concentrations of liposomes were estimated from the detected liposome number by FCM (FACSAria2; BD Biosciences) (10 μL/min at a flow rate of 1.0). Liposome solutions were mixed at the concentration or volume ratios presented in the text and then centrifuged at 18,000 × g for 5 min at 4 °C. Liposome solutions were then incubated at –196 °C (using liquid nitrogen) for 30 min in Fig. 1 and Figs. S1 and S5 *A and B* or 1 min in other experiments. Then, liposome solutions were thawed at room temperature for 10 min, resuspended, and centrifuged at 18,000 × g for 5 min at 4 °C. The supernatant was gently replaced with the same volume of new outer solution to wash out leaked materials from liposomes.

Rep-RNA Replication Inside Liposomes. The RNA encoding modified β-subunits of Qβ-replicase with enhanced replicability (35) was used as the template (2,041 bp) (Rep-RNA). The replication reaction of Rep-RNA in liposomes was performed at 37 °C using Rep-RNA and Qβ-replicase purified in our laboratory (44). Nutrients in liposomes required for RNA replication were set to fivefold higher concentrations than in the previous report (44) because we considered the leakage and diffusion of inner contents by F/T. RNA liposomes contained 125 mM Tris–HCl (pH 8.0), 25 mM MgCl$_2$, 0.01% BSA, 500 mM sucrose, 350 mM potassium glutamate, 50 mM Hepes–KOH (pH 7.6), and 5 nM Rep-RNA. Nutrient liposomes contained the same buffer, but replacing Rep-RNA with 6.25 mM of each NTP and 100 nM of purified Qβ-replicase.

Measuring RNA in Liposomes by SYBR. SYBR Green II was used to stain Rep-RNA in liposomes. Before measuring fluorescence by FCM or microscopy, SYBR Green II was added to the outer solution of liposomes to a final concentration of 1/10,000 the original and incubated for 10 min on ice. The Rep-RNA concentration (nM) in limited size liposomes (8,000–12,000 F.I. of ATTO633 measured by FCM) was calculated using the standard curve obtained in Fig. S2 by converting the SYBR fluorescence intensity as follows: Rep-RNA (nM) = 1.33 × SYBR F.I.

1. Szostak JW, Bartel DP, Luisi PL (2001) Synthesizing life. *Nature* 409(6818):387–390.
2. Monnard PA, Luptak A, Deamer DW (2007) Models of primitive cellular life: Polymerases and templates in liposomes. *Philos Trans R Soc Lond B Biol Sci* 362(1486):1741–1750.
3. Lane MD, Seelig B (2014) Advances in the directed evolution of proteins. *Curr Opin Chem Biol* 22:129–136.
4. Stano P, Luisi PL (2010) Achievements and open questions in the self-reproduction of vesicles and synthetic minimal cells. *Chem Commun (Camb)* 46(21):3639–3653.
5. Mills DR, Peterson RL, Spiegelman S (1967) An extracellular Darwinian experiment with a self-duplicating nucleic acid molecule. *Proc Natl Acad Sci USA* 58(1):217–224.
6. Noireaux V, Libchaber A (2004) A vesicle bioreactor as a step toward an artificial cell assembly. *Proc Natl Acad Sci USA* 101(51):17669–17674.
7. Kobori S, Ichihashi N, Kazuta Y, Yomo T (2013) A controllable gene expression system in liposomes that includes a positive feedback loop. *Mol Biosyst* 9(6):1282–1285.
8. Fenz SF, Sengupta K (2012) Giant vesicles as cell models. *Integr Biol (Camb)* 4(9):982–995.
9. Kita H, et al. (2008) Replication of genetic information with self-encoded replicase in liposomes. *ChemBioChem* 9(15):2403–2410.
10. Chakrabarti AC, Breaker RR, Joyce GF, Deamer DW (1994) Production of RNA by a polymerase protein encapsulated within phospholipid vesicles. *J Mol Evol* 39(6):555–559.
11. Blain JC, Szostak JW (2014) Progress toward synthetic cells. *Annu Rev Biochem* 83:615–640.
12. Zhu TF, Szostak JW (2009) Coupled growth and division of model protocell membranes. *J Am Chem Soc* 131(15):5705–5713.
13. Budin I, Debnath A, Szostak JW (2012) Concentration-driven growth of model protocell membranes. *J Am Chem Soc* 134(51):20812–20819.
14. Hanczyc MM, Fujikawa SM, Szostak JW (2003) Experimental models of primitive cellular compartments: Encapsulation, growth, and division. *Science* 302(5645):618–622.
15. Noireaux V, Maeda YT, Libchaber A (2011) Development of an artificial cell, from self-organization to computation and self-reproduction. *Proc Natl Acad Sci USA* 108(9):3473–3480.
16. Budin I, Szostak JW (2011) Physical effects underlying the transition from primitive to modern cell membranes. *Proc Natl Acad Sci USA* 108(13):5249–5254.
17. Takakura K, Toyota T, Sugawara T (2003) A novel system of self-reproducing giant vesicles. *J Am Chem Soc* 125(27):8134–8140.
18. Hardy MD, et al. (2015) Self-reproducing catalyst drives repeated phospholipid synthesis and membrane growth. *Proc Natl Acad Sci USA* 112(27):8187–8192.
19. Brea RJ, Cole CM, Devaraj NK (2014) In situ vesicle formation by native chemical ligation. *Angew Chem Int Ed Engl* 53(51):14102–14105.
20. Schmidli PK, Schurtenberger P, Luisi PL (1991) Liposome-mediated enzymatic synthesis of phosphatidylcholine as an approach to self-replicating liposomes. *J Am Chem Soc* 113(21):8127–8130.
21. Osawa M, Erickson HP (2013) Liposome division by a simple bacterial division machinery. *Proc Natl Acad Sci USA* 110(27):11000–11004.
22. Kurihara K, et al. (2011) Self-reproduction of supramolecular giant vesicles combined with the amplification of encapsulated DNA. *Nat Chem* 3(10):775–781.
23. Terasawa H, Nishimura K, Suzuki H, Matsuura T, Yomo T (2012) Coupling of the fusion and budding of giant phospholipid vesicles containing macromolecules. *Proc Natl Acad Sci USA* 109(16):5942–5947.
24. Boni LT, Stewart TP, Alderfer JL, Hui SW (1981) Lipid-polyethylene glycol interactions: I. Induction of fusion between liposomes. *J Membr Biol* 62(1-2):65–70.
25. Sunami T, et al. (2010) Detection of association and fusion of giant vesicles using a fluorescence-activated cell sorter. *Langmuir* 26(19):15098–15103.
26. Tanaka T, Yamazaki M (2004) Membrane fusion of giant unilamellar vesicles of neutral phospholipid membranes induced by La3+. *Langmuir* 20(13):5160–5164.
27. Tarahovsky YS, Yagolnik EA, Muzafarov EN, Abdrasilov BS, Kim YA (2012) Calcium-dependent aggregation and fusion of phosphatidylcholine liposomes induced by complexes of flavonoids with divalent iron. *Biochim Biophys Acta* 1818(3):695–702.
28. Toraya S, et al. (2005) Morphological behavior of lipid bilayers induced by melittin near the phase transition temperature. *Biophys J* 89(5):3214–3222.
29. Chan YH, van Lengerich B, Boxer SG (2009) Effects of linker sequences on vesicle fusion mediated by lipid-anchored DNA oligonucleotides. *Proc Natl Acad Sci USA* 106(4):979–984.
30. Costa AP, Xu X, Burgess DJ (2014) Freeze-anneal-thaw cycling of unilamellar liposomes: Effect on encapsulation efficiency. *Pharm Res* 31(1):97–103.
31. Anzai K, Yoshida M, Kirino Y (1990) Change in intravesicular volume of liposomes by freeze-thaw treatment as studied by the Esr stopped-flow technique. *Biochim Biophys Acta* 1021(1):21–26.
32. Pautot S, Frisken BJ, Weitz DA (2003) Production of unilamellar vesicles using an inverted emulsion. *Langmuir* 19(7):2870–2879.
33. Matosevic S (2012) Synthesizing artificial cells from giant unilamellar vesicles: State-of-the art in the development of microfluidic technology. *BioEssays* 34(11):992–1001.
34. Nishimura K, et al. (2012) Cell-free protein synthesis inside giant unilamellar vesicles analyzed by flow cytometry. *Langmuir* 28(22):8426–8432.
35. Ichihashi N, et al. (2013) Darwinian evolution in a translation-coupled RNA replication system within a cell-like compartment. *Nat Commun* 4:2494.
36. Fujii S, et al. (2014) Liposome display for in vitro selection and evolution of membrane proteins. *Nat Protoc* 9(7):1578–1591.
37. Nishimura K, et al. (2009) Population analysis of structural properties of giant liposomes by flow cytometry. *Langmuir* 25(18):10439–10443.
38. Zahnle K, Schaefer L, Fegley B (2010) Earth's earliest atmospheres. *Cold Spring Harb Perspect Biol* 2(10):a004895.
39. Oberholzer T, Wick R, Luisi PL, Biebricher CK (1995) Enzymatic RNA replication in self-reproducing vesicles: An approach to a minimal cell. *Biochem Biophys Res Commun* 207(1):250–257.
40. Mansy SS, et al. (2008) Template-directed synthesis of a genetic polymer in a model protocell. *Nature* 454(7200):122–125.
41. Kazuta Y, Matsuura T, Ichihashi N, Yomo T (2014) Synthesis of milligram quantities of proteins using a reconstituted in vitro protein synthesis system. *J Biosci Bioeng* 118(5):554–557.
42. Sunami T, Matsuura T, Suzuki H, Yomo T (2010) Synthesis of functional proteins within liposomes. *Methods Mol Biol* 607:243–256.
43. Chetverin AB, Chetverina HV, Demidenko AA, Ugarov VI (1997) Nonhomologous RNA recombination in a cell-free system: Evidence for a transesterification mechanism guided by secondary structure. *Cell* 88(4):503–513.
44. Kita H, et al. (2006) Functional Qbeta replicase genetically fusing essential subunits EF-Ts and EF-Tu with β-subunit. *J Biosci Bioeng* 101(5):421–426.

APPLIED BIOLOGICAL SCIENCES